Assessment of Temperature and Humidity Changes Associated With the September 2009 Dust Storm in Australia

Thomas A. Jones and Sundar A. Christopher

***Abstract*—A historic dust storm affected the eastern portions of Australia between 22 and 24 September 2009, causing significant reductions in air quality and visibility. Using multiple satellite remote sensing data sets and meteorological information, we assess the distribution of dust aerosols and their potential effects on the Earth-atmosphere system. Spaceborne active lidar data showed that dust aerosols were located up to 2 km above the surface. The thickness of the dust plume (0.55-μm aerosol optical thickness > 1.0) reduced surface visibility to below 2 km. Dew-point depressions of 20 °C or more occurred after passage of the dust plume, with decreases in surface temperature observed at some locations. Between the surface and 2-km level, temperature data show a cooling of $\sim$10 °C in the hours after passage of the cold front along which dust aerosols had converged. However, much of the temperature change that occurred is a result of cold air advection behind the northward traveling plume. Radiative transfer modeling suggests that only up to 1 °C per day of this cooling is due to the decrease in solar radiation reaching the surface layer. Radiative transfer modeling also indicates a net warming of up to 2 °C per day within and above the dust layer, possibly offsetting some cooling aloft due to the cold front passage. Modeling results indicate that expected aerosol radiative effects to temperature are small compared to synoptic influences and are unlikely to be sampled in observations under this scenario since the magnitudes of these effects are quite small.**

***Index Terms*—Aerosol, dust, humidity, Moderate Resolution Imaging SpectroRadiometer (MODIS), temperature, visibility.**

I. Introduction

DURING THE latter half of September 2009, the eastern portions of Australia were affected by a powerful dust storm that originated from south central Australia due to abnormally dry conditions present during the previous months. Impacts of this event included reduced visibility inhibiting transportation, closing schools and businesses, and lowering air quality to the extent that increases in respiratory distress were reported. Dust aerosols also have an impact on the surrounding atmospheric environment by modifying the temperature profile through scattering and absorption of solar and terrestrial radiation (e.g., [1] and [2]). Most aerosol types scatter solar radiation back into space, cooling the atmosphere below the layer where the aerosols exist. Due to their optical properties, dust aerosols also have the additional effect of warming the atmospheric layers near the surface through absorption and reemission of longwave radiation (e.g., [3]). The magnitude of this offset and the overall impact of dust aerosols to the atmosphere are highly dependent on their vertical distribution and concentration as well as the corresponding water vapor and surface albedo characteristics. Huang *et al.* [1] observed a warming of more than 3 °C per day in the layer where dust aerosols were present, generally 3–5 km above the surface during several events located in the Taklimakan Desert. The decrease in solar radiation reaching the surface cooled surface temperatures compared to aerosol-free regions, but the magnitude of this cooling was significantly less than that of the corresponding midtropospheric warming. Similar results have been observed pertaining to dust layers produced from the Saharan Desert and transported westward over the Atlantic Ocean or northward into the Mediterranean Sea (e.g., [2] and [4]). In most cases, the net effect of thick dust plumes is to cool the surface but warm the atmosphere aloft, with the warming effect being dominant when averaged from the surface to the tropopause.

In this letter, we use satellite remote sensing observations combined with meteorological observations and radiative transfer modeling of a dust outbreak in eastern Australia between 22 and 24 September 2009 to assess the atmospheric impacts of a quickly progressing dust plume. This dust storm occurred as a result of a deepening cyclone moving from southern Australia northeastward across the continent. Strong winds generated behind this system lofted large amounts of dust into the atmosphere and transported it northward while converging it along a cold front propagating northward with the cyclone. Cold air advection (CAA) behind the front brought cooler and dryer conditions into the region after passage of the dust plume. The circumstances surrounding this event are similar to those that produced another Australian dust storm on 23 October 2002 in the same region [5]. While the temperature and humidity changes due to synoptic effects are dominant, further changes caused by the presence of the dust aerosols may also occur, requiring further study.

Unlike some previous studies of dust aerosol radiative effects [1], [4], the dust layer does not remain present over one region for a prolonged amount of time (generally a week or more).

Manuscript received March 16, 2010; accepted July 22, 2010. This work was supported by the National Aeronautics and Space Administration's Radiation Sciences, Interdisciplinary Sciences, and ACMAP programs.

T. A. Jones is with the Earth System Science Center, The University of Alabama in Huntsville, Huntsville, AL 35805 USA (e-mail: tjones@nsstc.uah.edu).

S. A. Christopher is with the Earth System Science Center and Department of Atmospheric Science, The University of Alabama in Huntsville, Huntsville, AL 35805 USA.

Color versions of one or more of the figures in this paper are available online at http://ieeexplore.ieee.org.

Digital Object Identifier 10.1109/LGRS.2010.2063693

Therefore, atmospheric effects associated with the dust are likely to be smaller and more transient in space and time. Using multiple data sources, we track the dust plume and assess corresponding atmospheric conditions to determine the relationship between the two. We also assess whether these changes are due to aerosol radiative effects or simply due to the advection of different air masses into a particular location. The goal is to examine the characteristics of the dust storm using satellite- and surface-based observations in addition to radiative transfer modeling analysis to determine what, if any, measurable effects that the dust aerosols had on surface and midtropospheric conditions.

II. Data

The Moderate Resolution Imaging SpectroRadiometer (MODIS) on the Terra and Aqua satellites measures reflected and emitted radiation from the Earth-atmosphere system in 36 spectral channels between 0.405 and 14.385 μm, with a swath width of 2330 km providing a near daily global coverage. Calibrated Level 1B data have a spatial resolution of 0.25–1 km, which are used by this letter to show the locations of the dust storm and surrounding atmospheric features. The level 2 (L2) aerosol optical thickness (AOT) product (collection 5) is generated at a 10-km^2 resolution using a set of 20 $\times$ 20 (400) 0.5-km-resolution visible and 10 $\times$ 10 (100) 1.0-km-resolution near-IR radiances. This product represents a total columnar value of aerosol extinction and allows for global mapping of aerosol loading from space [6]. MODIS data used here are collected from Aqua for 22–24 September, with the overpass time over this region occurring between 0300 and 0600 UTC each day. Terra data, whose overpass time is $\sim$3 h earlier, were also collected, but dust plume characteristics from it were very similar to Aqua observations; thus, only the latter are shown as part of this discussion. The vertical profile of the dust aerosols is obtained from a CALIPSO overpass at 1500 UTC on 23 September. The CALIOP sensor onboard the CALIPSO satellite is an active lidar providing vertical profiles of backscatter at 532 and 1064 nm as well as the parallel and perpendicularly polarized components of 532-nm backscatter. These data sample the vertical distribution of atmospheric clouds and aerosols along with particle shape characteristics [7]. In this letter, we use the level 1, version 3.01, backscatter and depolarization products at 532 nm.

Atmospheric data are acquired from surface and radiosonde stations located in this region as well as from numerical model analyses. Surface observations are available every 30 min and include temperature, humidity, pressure, wind speed (sustained and gusts) and direction, and visibility. The National Centers for Environmental Prediction's Global Forecast System (GFS) model analysis data [8] are used to assess atmospheric conditions above the surface, since radiosonde data corresponding to this event are sparse. The GFS model provides global meteorological conditions with a 0.5° horizontal resolution and a 9 pressure-level vertical resolution between the surface and 700 hPa produced at 6-h time intervals. We primarily use the 850-hPa temperature data, which are near the level of the dust aerosols, to assess the impact of the frontal passage and dust aerosols on low- to midtropospheric atmospheric conditions.

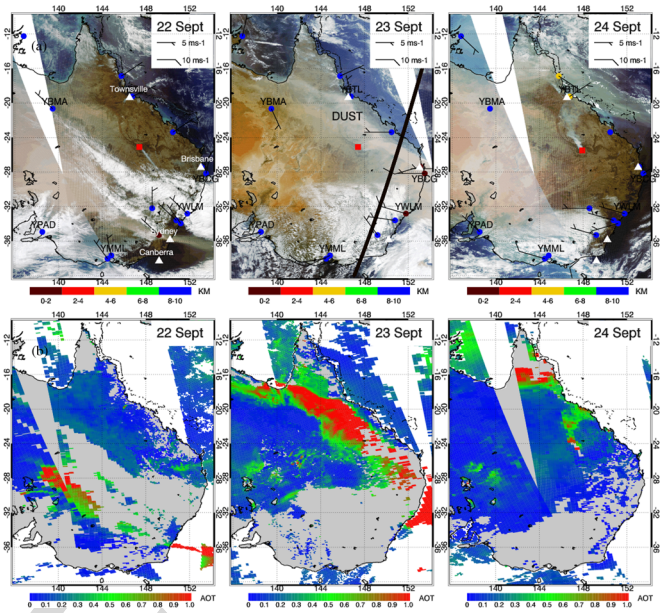

Fig. 1. (a) True-color Aqua MODIS imagery from 22 to 24 September 2009. Surface observation sites are shown with wind barbs (see legend), with colors representing visibility at the overpass time. Blue color represents visibility greater than 8 km, while red colors represent visibilities less than 4 km. The red square denotes the location of the origin of a smoke plume observed during this event. The CALIPSO overpass location is given by black line on 23 September on the relevant panel. (b) MODIS AOT at 0.55 μm for the same times as in panel (a). Note the lack of AOT retrievals where dust aerosol concentration is greatest.

III. Discussion

The dust plume is evident from Aqua MODIS 1-km RGB color composite using red (0.67 μm), green (0.55 μm), and blue (0.47 μm) 1-km data between 22 and 24 September 2009, beginning in central and southern Australia on 22 September and quickly moving north and into the Coral Sea by 24 September [Fig. 1(a)]. The dust aerosols originate from the dry interior of the continent and are initially transported eastward by a deepening cyclone, forming a long and narrow dust plume over southeastern Australia on 22 September. One day later, the plume has moved northward and broadened to cover a much larger area affecting the towns of Sydney, Brisbane, and eventually Townsville along the northern coast, causing significant reductions in air quality and visibility [Fig. 1(a)]. By 24 September, most of the dust has been transported off the coast, greatly improving conditions over much of eastern Australia. MODIS also shows a small but persistent smoke plume originating near $-25°$ S and 147° E. Note that the smoke is being transported in a southeasterly direction early on 22 September, but in a northerly direction by 24 September, corresponding well to the evolution of the dust plume. MODIS AOT at 0.55 μm showed a similar pattern with the maximum values (AOT $>$ 1.0) corresponding to the dust aerosols present on the visible imagery [Fig. 1(b)]. However, AOT retrievals were often not made in the most intense portions of the dust plume due to the retrieval algorithms misclassifying the optically thick aerosols as clouds [9].

The complex characteristics of this dust plume are evident from the CALIPSO backscatter profiles [Fig. 2(a)] at approximately 1500 UTC on 23 September [or $\sim$12 h after the corresponding MODIS image from Aqua in Fig. 1(a)]. Very

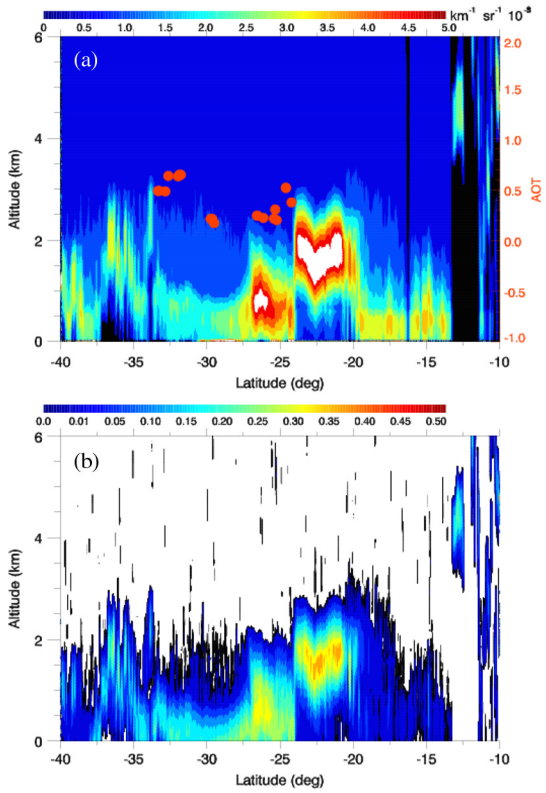

Fig. 2. (a) CALIPSO backscatter at 532 nm at ∼1500 UTC, 23 September, along the path denoted in Fig. 1(a). Also shown is AOT at 0.55 μm from the Aqua overpass at ∼0400 UTC (right axis). Note the temporal lag between the dust signatures from CALIPSO and MODIS observations owing to the rapid transit of the dust northward. (b) Corresponding CALIPSO depolarization ratio, with the highest values corresponding to the nonspherical dust particles within the plume.

high backscatter at 532 nm is present in two distinct regions. The first is located below 1 km above the surface between -28° and -24° S, and the second is further northward from -24° to -19° S at between 1.5 and 2 km above the surface. Both maxima in backscattering are a result of dust aerosols, and the rapid change in aerosol layer height is quite interesting. We are confident that both layers represent dust aerosols since the CALIPSO depolarization ratio (perpendicular 532-nm backscatter/parallel 532-nm backscatter) is greater than 0.4 [Fig. 2(b)]. Recall that dust aerosols are often nonspherical in nature and thus will cause a higher depolarization ratio compared to more spherical aerosol types and/or cloud water droplets. Comparing the CALIPSO data to the Aqua overpass 12 h prior [Fig. 1(a)], we see that the higher elevation portion of the dust plume likely corresponds to the relatively narrow but very apparent dust plume northwest of YBCG. MODIS AOTs along the CALIPSO path 12 h prior are approximately 0.5 for both dust layers [Fig. 2(a)]. The apparent offset between maximum AOT and 532-nm backscatter is likely due to the ∼12-h difference in observation times. Still, the spatial extent of the dust plume is consistent at about 7° from south to north. It would appear that the major dust plume was being transported rapidly northward along a cold front. Along the front, dust aerosols were being transported upward and over the surface boundary as it continued to push northward. Behind the front, dust became trapped in the sinking air in its wake and, as a result, was transported downward toward the surface.

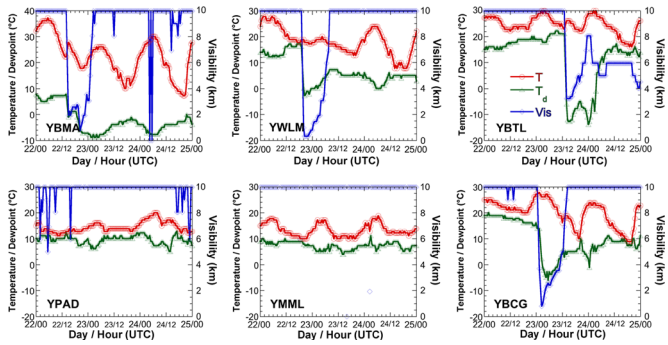

Fig. 3. (Red) Surface temperature, (green) dew point, and (blue) visibility for six measurement stations in Australia whose locations are shown in Fig. 1.

The spatial and temporal evolution of the dust plume was also noted from atmospheric observations. Time series of surface visibility is plotted for several stations in the domain of study (Fig. 3). Visibility was poor ($<$ 2 km) at only a single station in southeast on 22 September corresponding to the location of the narrow but thick dust plume. By the next day, poor visibility conditions existed at several stations along the eastern coast, including YBCG and YWLM. At the southern-most station (YWLM), visibility decreased rapidly around 2000 UTC on 22 September before improving almost as quickly around 0600 UTC on 23 September as the plume passed by. Further north at YBCG, a similar trend was observed, but occurring several hours later. Dust did not reach the northern-most station (YBTL) until 1200 UTC 23 September, with low visibility continuing until after 0000 UTC 24 September. A brief improvement in visibility occurred near 0000 UTC 25 September, but decreased again thereafter. The reason for this secondary decrease, which was not observed at any other site, was due to advection of smoke from the ongoing fire located to the south (Figs. 1 and 3).

Further westward and further inland, station YBMA reported a decrease in visibility between 1200 UTC 22 September and 0000 UTC 23 September. The dust plume reached this location prior to those stations further east as YBMA was much nearer the dust source regions in western New South Wales. At all these locations, the sky was observed to turn an orange-red color with a significant reduction in solar radiation reaching the surface being readily apparent. Along the southern coast of Australia at YMML and YPAD, no dust signature is present in the surface visibility or humidity data, indicating that all dust associated with this event is being transported north and northeastward away from these locations. The overall lag in visibility change from south to north allows us to estimate the speed at which the dust plume was moving northward and dispersing. Using the time of the initial drop in visibility as a guide, we find that the dust plume was traveling northward at speeds in excess of 20 $\mathrm{m \cdot s^{-1}}$, meaning that it traversed the continent in less than two days.

One goal of this work is to determine the magnitude of the dust aerosol radiative effects and whether they can be recorded using observational data. It has been shown through observational and modeling studies that dust aerosols can either cool or warm the atmosphere depending upon surface albedo, water vapor, and dust aerosol properties [2], [10], [11]. Observations from ground instruments near Sydney noted a maximum in the

particle size distribution between 1.0 and 10.0 μm, with total particle mass concentrations (all sizes) of up to 578 $\mu g \cdot m^{-3}$ and mineral type mostly composed of silicates [12]. Yang *et al.* [11] noted that, for surface albedo greater than approximately 0.35, the shortwave cooling transitions to surface warming due to increased scattering between surface and aerosol layer. However, this threshold was not reached at the coastal sites of YBCG, YBTL, and YWLM where surface albedos from MODIS are only between 0.05 and 0.08. Therefore, a cooling effect at the surface is expected at these observation sites. Further inland near YBMA, the surface albedo was 0.1 but increased to near 0.25 near the dust source. Only in this location may warming come close to overwhelming surface cooling.

To determine if we are seeing aerosol radiative effects in this example, we first analyze the time series of temperature and dew point from six observation sites throughout central and eastern Australia (Figs. 1 and 3). For stations YBTL, YBCG, YWLM, and YBMA, a large decrease in dew point occurred at the same time as the decrease in visibility noted earlier (Fig. 3). The primary cause of the decrease in temperature and humidity is the advection of a cooler and dryer airmass into these areas after passage of the cold front (along which the dust aerosols have converged). Several previous studies have also noted the apparent collocation of dust aerosols and dry air (e.g., [13]), which is consistent with the dryer air generally present near the source regions of dust aerosols. The relationship between dust aerosols and surface temperature is not readily apparent. Along the east coast of Australia, the average diurnal temperature change during this time period has the maximum temperatures occurring around 0400 UTC with minimums occurring around 2000 UTC. The most apparent change in temperature corresponding to the arrival of the dust plume occurs at YBCG (Fig. 3). During the first hour after the rapid decrease in surface visibility, a temperature rise of approximately 7 °C was observed, followed by a surface temperature decrease of more than 10 °C during the following 8-h period between 0400 UTC and 1200 UTC. The average diurnal temperature change cannot account for these differences as it was a total of ~ 5 °C the day before. The spike in temperature at the moment of arrival of the dust plume is very interesting and could be a result of the convergence of warm air just ahead of the cold front and its associated dust plume. However, the CAA behind the cold front quickly reduces temperature, and it continues to decrease after 1400 UTC when visibility returned to normal. The primary source for the cooler air lies in southern Australia and corresponds to a region of persistent cloud cover that exists between 22 and 24 September, which can be seen in Fig. 1(a). The cloud cover acts to cool the surface compared to clear-sky conditions, and since they lie behind the cold front, they are likely to increase the strength of the cold pool of air being advected northward.

A similar pattern of rapid warming of 5 °C, followed by cooling of > 10 °C, was also observed further west at YBMA, indicating similar synoptic conditions present along much of the frontal boundary. Unlike YBCG, surface temperature appeared to recover somewhat around the time visibility improved before rapidly decreasing again. However, this secondary decrease was primarily due to the onset of nightfall and loss of solar radiation

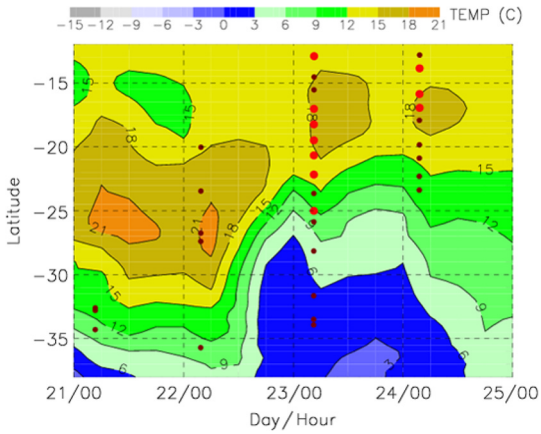

Fig. 4. GFS 850-hPa temperature (in degree Celsius) zonally averaged between 142° and 152° E every 6 h between 21 and 25 September. Locations where Aqua AOT > 0.5 along this path are plotted in maroon, and those where AOT > 1.0 are plotted in red.

at the surface. Interestingly, temperature anomalies at the other two eastern Australian stations of YBTL and YWLM were much smaller despite the presence of the visibility and dew-point signatures corresponding to the passage of the dust plume and cold front. At YWLM, cloud cover is present until 24 September, limiting potential temperature changes from either dust aerosols or passage of the cold front. Further west at YBTL, the thickness of the dust plume and strength of the cold front were weakest, producing more limited temperature changes. In addition, the impact of smoke from the ongoing fire to the south of this site could be influencing atmospheric characteristics.

Above the surface layer, larger temperature changes appear to occur corresponding to the passage of the dust plume. Fig. 4 shows the GFS 850-hPa temperature zonally averaged between 142° and 152° E at six-hourly intervals between 21 and 25 September. This level roughly corresponds to the height of the initial dust plume seen on the CALIPSO data in Fig. 2(a). Also shown are locations and times where AOT > 0.5 or > 1.0 from MODIS across the same region. The AOT data show that the concentration of dust aerosols increases significantly from 21 to 23 September, with the area between $-27°$ and $-17°$ S often having AOT > 1.0 at the latter date. The northward movement of the dust plume can also be seen, with the maximum AOT values spreading northward as a function of time, while high AOT values further southward become less common, with no AOT > 0.5 below $-25°$ S by 24 September.

A major temperature change event occurs after 1200 UTC 22 September. Temperature at 850 hPa decreased by over 10 °C over a period of less than 6 h between $-35°$ and $-28°$ S. Radiosonde data from near Brisbane were consistent with the GFS model output. The cold pool remained in place until at least 1200 UTC 24 September. Further north, temperatures remain warmer, mostly > 15 °C. Temperatures throughout the 1000–850-hPa layer generally cool from south to north in the eastern half of Australia, with cooling generally occurring behind the initial band of thick dust noted in Fig. 1(a). From these data, it is clear that cooling temperatures follow behind the dust plume, while a temperature maximum seems to exist near the location of the highest AOT values just prior to initial passage of the boundary (and consistent with the temperature

rise observed at this time from several surface stations). Even though we are likely seeing a dust-induced cooling event at the surface and aloft, it is only a small part of the overall surface temperature trends present. How small requires the use of radiative transfer modeling to estimate temperature changes given the observed aerosol properties.

To better estimate the amount of temperature change occurring as a result of *only* dust aerosol radiative effects, we use Fu-Liou radiative transfer model output [14] combined with the observed dust aerosol and surface albedo properties from MODIS and CALIPSO. Aerosol and aerosol-free fluxes are computed at the location of each surface station shown in Fig. 1 near the time corresponding to the sharp decrease in observed surface visibility. No computation is made for the two sites (YMML and YPAD) where no significant change in visibility was observed. Modeling results indicate a net (SW+LW) cooling rate of less than 1 °C per day at the surface up to the dust layer for the four remaining locations. Above the aerosol layer at 2 km, a warming rate of up to 2 °C per day was estimated. These values are much smaller than the observed temperature changes, particularly considering that the estimate heating or cooling rates are less than 2 °C *for an entire one-day period*. It is possible that the radiative transfer model is somewhat underestimating the aerosol effects, but even a doubling of the model estimate would not come close to explaining the temperature trends observed in the data. Thus, it is clear that dust aerosol radiative effects only contribute a small portion of the temperature changes being observed during this event. Synoptic effects such as CAA behind a rapidly propagating cold front are the dominant factor in temperature trends being observed, with dust radiative effects only acting to reenforce what is already happening. Much higher resolution atmospheric modeling data are required along with models that can be run with and without the dust storm occurring to close the loop on precisely quantifying this relationship for dust storms such as these.

IV. Conclusion

Analysis of the 22–24 September 2009 dust storm in eastern Australia has revealed several interesting phenomena associated with dust aerosols and the surrounding environment. The progression of this historic dust storm was evident from satellite-based sensors such as MODIS and CALIPSO. These observations showed the northward progression of a dust storm through central Australia and eventually toward New Zealand. The dust aerosol layer height was not constant and was greatest along the leading edge of the dust (2 km) and decreased in height further southward (< 1 km). This change in dust height was attributed to the rapid movement of the cold front and convergence of the dust along and over the cool pool of air as it progressed northward.

Meteorological observations also show the progression of the cold front and dust plume, primarily in the form of rapid decreases in atmospheric humidity and visibility. Dew point decreased more than 20 °C at YBTL and YCBG with visibilities dropping to below 2 km in some instances from the clear-sky value of 10 km. A sudden increase followed by a longer decrease in surface temperature was observed at two sites (YBML and YBCG) after the passage of the initial dust plume. A similar decrease occurred aloft near 850 hPa following passage of the dust layer. However, no surface temperature change was observed at other locations such as YBTL calling into question the significance of possible aerosol radiative effects in this example. Radiative transfer modeling indicates a dust aerosol radiative effect on the order of 1 or 2 °C per day, which represents a change temperature an order of magnitude smaller than measured. The primary factor in the changing surface conditions appears to be a result of the passage of the surface cold front and CAA behind it. However, surface layer cooling due to dust aerosol radiative effects may very well be reenforcing the cold pool as it progressed northward. Future research will assess this question using more dust storm examples coupled with mesoscale modeling comparisons to better quantify the effects of dust storms on surrounding atmospheric conditions.

Acknowledgment

The CALIPSO data were obtained through the NASA Langley Distributed Active Archive Systems, and the MODIS data were obtained from the Atmospheric Archive and Distribution System.

References

[1] J. Huang, Q. Fu, J. Su, Q. Tang, P. Minnis, Y. Yi, and Q. Zhao, "Taklimakan dust aerosol radiative heating derived from CALIPSO observations using Fu-Liou radiation model with CERES constraints," *Atmos. Chem. Phys.*, vol. 9, no. 12, pp. 4011–4021, Jun. 2009.

[2] C. Perez, S. Nickovic, G. Pejanovic, J. M. Baldasano, and E. Ozsoy, "Interactive dust-radiation modeling: A step to improve weather forecasts," *J. Geophys. Res.*, vol. 111, p. D16 206, 2006, DOI: 10.1029/2005JD006717.

[3] S. A. Christopher and T. A. Jones, "Dust radiative effect over global oceans," *IEEE Geosci. Remote Sens. Lett.*, vol. 5, no. 1, pp. 74–77, Jan. 2008.

[4] A. Zhu, V. Ramanathan, F. Li, and D. Kim, "Dust plumes over the Pacific, Indian, and Atlantic oceans: Climatology and radiative impact," *J. Geophys. Res.*, vol. 112, p. D16 208, 2007, DOI: 10.1029/2007JD008427.

[5] G. McTainsh, Y. C. Chan, H. McGowan, J. Leys, and K. Tews, "The 23rd October 2002 dust storm in eastern Australia: Characteristics and meteorological conditions," *Atmos. Environ.*, vol. 39, no. 7, pp. 1227–1236, Mar. 2005.

[6] L. A. Remer, R. G. Kleidman, R. C. Levy, Y. J. Kaufman, D. Tanré, S. Mattoo, J. V. Martins, C. Ichoku, I. Koren, H. Yu, and B. N. Holben, "Global aerosol climatology from the MODIS satellite sensors," *J. Geophys. Res.*, vol. 113, p. D14 S07, 2008, DOI: 10.1029/2007JD009661.

[7] M. Vaughan, S. Young, D. Winker, K. Powell, A. Omar, Z. Liu, Y. Hu, and C. Hostetler, "Fully automated analysis of space-based lidar data: An overview of the CALIPSO retrieval algorithms and data products," *Proc. SPIE*, vol. 5575, pp. 16–30, 2004.

[8] S. Moorthi, H.-L. Pan, and P. Caplan, Changes to the 2001 NCEP operational MRF/AVN global analysis/forecast system, Silver Spring, MD, 2001, Tech. Procedures Bull. 484, 14 pp. [Online]. Available: http://205.156.54.206/om/tpb/484.htm

[9] J. I. Brennan, Y. J. Kaufman, I. Koren, and R.-R. Li, "Aerosol–cloud interaction—Misclassi?cation of MODIS clouds in heavy aerosol," *IEEE Trans. Geosci. Remote Sens.*, vol. 43, no. 4, pp. 911–915, Apr. 2005.

[10] F. Patadia, E. Yang, and S. A. Christopher, "Does dust change the clear sky top of atmosphere shortwave flux over high surface reflectance regions?" *Geophys. Res. Lett.*, vol. 36, p. L15 825, 2009, DOI: 10.1029/2009GL039092.

[11] E. Yang, P. Gupta, and S. A. Christopher, "Net radiative effect of dust aerosols from satellite measurements over Sahara," *Geophys. Res. Lett.*, vol. 36, p. L18 812, 2009, DOI: 10.1029/2009GL039801.

[12] M. Radhi, M. A. Box, G. P. Box, and D. D. Cohen, "Size-resolved chemical composition of the Sydney dust storm," *J. Air Quality Clim. Change*, 2010, submitted for publication. AQ5

[13] J. P. Dunion and C. S. Velden, "The impact of the Saharan air layer on Atlantic tropical cyclone activity," *Bull. Amer. Meteorol. Soc.*, vol. 85, no. 3, pp. 353–365, Mar. 2004.

[14] Q. Fu and K. N. Liou, "Parameterization of the radiative effect properties of cirrus clouds," *J. Atmos. Sci.*, vol. 50, no. 13, pp. 2008–2025, Jul. 1993.

AUTHOR QUERIES

AUTHOR PLEASE ANSWER ALL QUERIES

AQ1 = Occurrences of "day^{-1}" were changed to "per day." Please check if OK.
AQ2 = Please provide the expanded form of the acronym "ACMAP" if applicable.
AQ3 = Please check if the intended meaning of the sentence was retained.
AQ4 = Please check if the intended meaning of the sentence was retained.
AQ5 = Please provide publication update in Ref. [12].

END OF ALL QUERIES

Assessment of Temperature and Humidity Changes Associated With the September 2009 Dust Storm in Australia

Thomas A. Jones and Sundar A. Christopher

***Abstract*—A historic dust storm affected the eastern portions of Australia between 22 and 24 September 2009, causing significant reductions in air quality and visibility. Using multiple satellite remote sensing data sets and meteorological information, we assess the distribution of dust aerosols and their potential effects on the Earth-atmosphere system. Spaceborne active lidar data showed that dust aerosols were located up to 2 km above the surface. The thickness of the dust plume (0.55-μm aerosol optical thickness > 1.0) reduced surface visibility to below 2 km. Dew-point depressions of 20 °C or more occurred after passage of the dust plume, with decreases in surface temperature observed at some locations. Between the surface and 2-km level, temperature data show a cooling of $\sim$10 °C in the hours after passage of the cold front along which dust aerosols had converged. However, much of the temperature change that occurred is a result of cold air advection behind the northward traveling plume. Radiative transfer modeling suggests that only up to 1 °C per day of this cooling is due to the decrease in solar radiation reaching the surface layer. Radiative transfer modeling also indicates a net warming of up to 2 °C per day within and above the dust layer, possibly offsetting some cooling aloft due to the cold front passage. Modeling results indicate that expected aerosol radiative effects to temperature are small compared to synoptic influences and are unlikely to be sampled in observations under this scenario since the magnitudes of these effects are quite small.**

***Index Terms*—Aerosol, dust, humidity, Moderate Resolution Imaging SpectroRadiometer (MODIS), temperature, visibility.**

I. Introduction

DURING THE latter half of September 2009, the eastern portions of Australia were affected by a powerful dust storm that originated from south central Australia due to abnormally dry conditions present during the previous months. Impacts of this event included reduced visibility inhibiting transportation, closing schools and businesses, and lowering air quality to the extent that increases in respiratory distress were reported. Dust aerosols also have an impact on the surrounding atmospheric environment by modifying the temperature profile through scattering and absorption of solar and terrestrial radiation (e.g., [1] and [2]). Most aerosol types scatter solar radiation back into space, cooling the atmosphere below the layer where the aerosols exist. Due to their optical properties, dust aerosols also have the additional effect of warming the atmospheric layers near the surface through absorption and reemission of longwave radiation (e.g., [3]). The magnitude of this offset and the overall impact of dust aerosols to the atmosphere are highly dependent on their vertical distribution and concentration as well as the corresponding water vapor and surface albedo characteristics. Huang *et al.* [1] observed a warming of more than 3 °C per day in the layer where dust aerosols were present, generally 3–5 km above the surface during several events located in the Taklimakan Desert. The decrease in solar radiation reaching the surface cooled surface temperatures compared to aerosol-free regions, but the magnitude of this cooling was significantly less than that of the corresponding midtropospheric warming. Similar results have been observed pertaining to dust layers produced from the Saharan Desert and transported westward over the Atlantic Ocean or northward into the Mediterranean Sea (e.g., [2] and [4]). In most cases, the net effect of thick dust plumes is to cool the surface but warm the atmosphere aloft, with the warming effect being dominant when averaged from the surface to the tropopause.

In this letter, we use satellite remote sensing observations combined with meteorological observations and radiative transfer modeling of a dust outbreak in eastern Australia between 22 and 24 September 2009 to assess the atmospheric impacts of a quickly progressing dust plume. This dust storm occurred as a result of a deepening cyclone moving from southern Australia northeastward across the continent. Strong winds generated behind this system lofted large amounts of dust into the atmosphere and transported it northward while converging it along a cold front propagating northward with the cyclone. Cold air advection (CAA) behind the front brought cooler and dryer conditions into the region after passage of the dust plume. The circumstances surrounding this event are similar to those that produced another Australian dust storm on 23 October 2002 in the same region [5]. While the temperature and humidity changes due to synoptic effects are dominant, further changes caused by the presence of the dust aerosols may also occur, requiring further study.

Unlike some previous studies of dust aerosol radiative effects [1], [4], the dust layer does not remain present over one region for a prolonged amount of time (generally a week or more).

Manuscript received March 16, 2010; accepted July 22, 2010. This work was supported by the National Aeronautics and Space Administration's Radiation Sciences, Interdisciplinary Sciences, and ACMAP programs.

T. A. Jones is with the Earth System Science Center, The University of Alabama in Huntsville, Huntsville, AL 35805 USA (e-mail: tjones@nsstc.uah.edu).

S. A. Christopher is with the Earth System Science Center and Department of Atmospheric Science, The University of Alabama in Huntsville, Huntsville, AL 35805 USA.

Color versions of one or more of the figures in this paper are available online at http://ieeexplore.ieee.org.

Digital Object Identifier 10.1109/LGRS.2010.2063693

Therefore, atmospheric effects associated with the dust are likely to be smaller and more transient in space and time. Using multiple data sources, we track the dust plume and assess corresponding atmospheric conditions to determine the relationship between the two. We also assess whether these changes are due to aerosol radiative effects or simply due to the advection of different air masses into a particular location. The goal is to examine the characteristics of the dust storm using satellite- and surface-based observations in addition to radiative transfer modeling analysis to determine what, if any, measurable effects that the dust aerosols had on surface and midtropospheric conditions.

II. Data

The Moderate Resolution Imaging SpectroRadiometer (MODIS) on the Terra and Aqua satellites measures reflected and emitted radiation from the Earth-atmosphere system in 36 spectral channels between 0.405 and 14.385 μm, with a swath width of 2330 km providing a near daily global coverage. Calibrated Level 1B data have a spatial resolution of 0.25–1 km, which are used by this letter to show the locations of the dust storm and surrounding atmospheric features. The level 2 (L2) aerosol optical thickness (AOT) product (collection 5) is generated at a 10-km^2 resolution using a set of 20 $\times$ 20 (400) 0.5-km-resolution visible and 10 $\times$ 10 (100) 1.0-km-resolution near-IR radiances. This product represents a total columnar value of aerosol extinction and allows for global mapping of aerosol loading from space [6]. MODIS data used here are collected from Aqua for 22–24 September, with the overpass time over this region occurring between 0300 and 0600 UTC each day. Terra data, whose overpass time is $\sim$3 h earlier, were also collected, but dust plume characteristics from it were very similar to Aqua observations; thus, only the latter are shown as part of this discussion. The vertical profile of the dust aerosols is obtained from a CALIPSO overpass at 1500 UTC on 23 September. The CALIOP sensor onboard the CALIPSO satellite is an active lidar providing vertical profiles of backscatter at 532 and 1064 nm as well as the parallel and perpendicularly polarized components of 532-nm backscatter. These data sample the vertical distribution of atmospheric clouds and aerosols along with particle shape characteristics [7]. In this letter, we use the level 1, version 3.01, backscatter and depolarization products at 532 nm.

Atmospheric data are acquired from surface and radiosonde stations located in this region as well as from numerical model analyses. Surface observations are available every 30 min and include temperature, humidity, pressure, wind speed (sustained and gusts) and direction, and visibility. The National Centers for Environmental Prediction's Global Forecast System (GFS) model analysis data [8] are used to assess atmospheric conditions above the surface, since radiosonde data corresponding to this event are sparse. The GFS model provides global meteorological conditions with a 0.5° horizontal resolution and a 9 pressure-level vertical resolution between the surface and 700 hPa produced at 6-h time intervals. We primarily use the 850-hPa temperature data, which are near the level of the dust aerosols, to assess the impact of the frontal passage and dust aerosols on low- to midtropospheric atmospheric conditions.

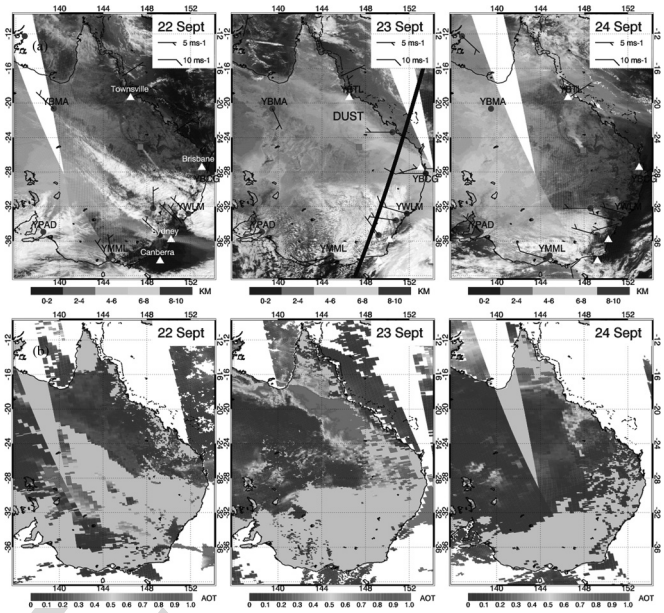

Fig. 1. (a) True-color Aqua MODIS imagery from 22 to 24 September 2009. Surface observation sites are shown with wind barbs (see legend), with colors representing visibility at the overpass time. Blue color represents visibility greater than 8 km, while red colors represent visibilities less than 4 km. The red square denotes the location of the origin of a smoke plume observed during this event. The CALIPSO overpass location is given by black line on 23 September on the relevant panel. (b) MODIS AOT at 0.55 μm for the same times as in panel (a). Note the lack of AOT retrievals where dust aerosol concentration is greatest.

III. Discussion

The dust plume is evident from Aqua MODIS 1-km RGB color composite using red (0.67 μm), green (0.55 μm), and blue (0.47 μm) 1-km data between 22 and 24 September 2009, beginning in central and southern Australia on 22 September and quickly moving north and into the Coral Sea by 24 September [Fig. 1(a)]. The dust aerosols originate from the dry interior of the continent and are initially transported eastward by a deepening cyclone, forming a long and narrow dust plume over southeastern Australia on 22 September. One day later, the plume has moved northward and broadened to cover a much larger area affecting the towns of Sydney, Brisbane, and eventually Townsville along the northern coast, causing significant reductions in air quality and visibility [Fig. 1(a)]. By 24 September, most of the dust has been transported off the coast, greatly improving conditions over much of eastern Australia. MODIS also shows a small but persistent smoke plume originating near $-25°$ S and 147° E. Note that the smoke is being transported in a southeasterly direction early on 22 September, but in a northerly direction by 24 September, corresponding well to the evolution of the dust plume. MODIS AOT at 0.55 μm showed a similar pattern with the maximum values (AOT > 1.0) corresponding to the dust aerosols present on the visible imagery [Fig. 1(b)]. However, AOT retrievals were often not made in the most intense portions of the dust plume due to the retrieval algorithms misclassifying the optically thick aerosols as clouds [9].

The complex characteristics of this dust plume are evident from the CALIPSO backscatter profiles [Fig. 2(a)] at approximately 1500 UTC on 23 September [or $\sim$12 h after the corresponding MODIS image from Aqua in Fig. 1(a)]. Very

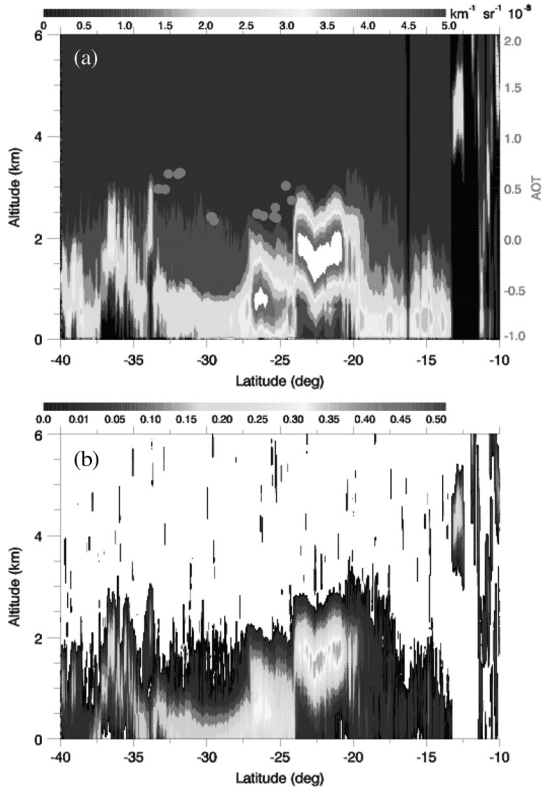

Fig. 2. (a) CALIPSO backscatter at 532 nm at ∼1500 UTC, 23 September, along the path denoted in Fig. 1(a). Also shown is AOT at 0.55 μm from the Aqua overpass at ∼0400 UTC (right axis). Note the temporal lag between the dust signatures from CALIPSO and MODIS observations owing to the rapid transit of the dust northward. (b) Corresponding CALIPSO depolarization ratio, with the highest values corresponding to the nonspherical dust particles within the plume.

high backscatter at 532 nm is present in two distinct regions. The first is located below 1 km above the surface between -28° and -24° S, and the second is further northward from -24° to -19° S at between 1.5 and 2 km above the surface. Both maxima in backscattering are a result of dust aerosols, and the rapid change in aerosol layer height is quite interesting. We are confident that both layers represent dust aerosols since the CALIPSO depolarization ratio (perpendicular 532-nm backscatter/parallel 532-nm backscatter) is greater than 0.4 [Fig. 2(b)]. Recall that dust aerosols are often nonspherical in nature and thus will cause a higher depolarization ratio compared to more spherical aerosol types and/or cloud water droplets. Comparing the CALIPSO data to the Aqua overpass 12 h prior [Fig. 1(a)], we see that the higher elevation portion of the dust plume likely corresponds to the relatively narrow but very apparent dust plume northwest of YBCG. MODIS AOTs along the CALIPSO path 12 h prior are approximately 0.5 for both dust layers [Fig. 2(a)]. The apparent offset between maximum AOT and 532-nm backscatter is likely due to the ∼12-h difference in observation times. Still, the spatial extent of the dust plume is consistent at about 7° from south to north. It would appear that the major dust plume was being transported rapidly northward along a cold front. Along the front, dust aerosols were being transported upward and over the surface boundary as it continued to push northward. Behind the front, dust became trapped in the sinking air in its wake and, as a result, was transported downward toward the surface.

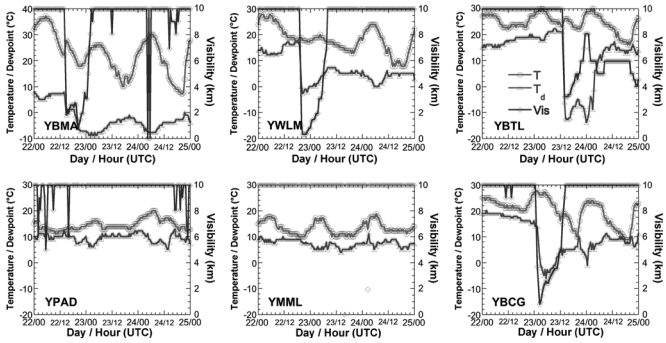

Fig. 3. (Red) Surface temperature, (green) dew point, and (blue) visibility for six measurement stations in Australia whose locations are shown in Fig. 1.

The spatial and temporal evolution of the dust plume was also noted from atmospheric observations. Time series of surface visibility is plotted for several stations in the domain of study (Fig. 3). Visibility was poor ($<$ 2 km) at only a single station in southeast on 22 September corresponding to the location of the narrow but thick dust plume. By the next day, poor visibility conditions existed at several stations along the eastern coast, including YBCG and YWLM. At the southern-most station (YWLM), visibility decreased rapidly around 2000 UTC on 22 September before improving almost as quickly around 0600 UTC on 23 September as the plume passed by. Further north at YBCG, a similar trend was observed, but occurring several hours later. Dust did not reach the northern-most station (YBTL) until 1200 UTC 23 September, with low visibility continuing until after 0000 UTC 24 September. A brief improvement in visibility occurred near 0000 UTC 25 September, but decreased again thereafter. The reason for this secondary decrease, which was not observed at any other site, was due to advection of smoke from the ongoing fire located to the south (Figs. 1 and 3).

Further westward and further inland, station YBMA reported a decrease in visibility between 1200 UTC 22 September and 0000 UTC 23 September. The dust plume reached this location prior to those stations further east as YBMA was much nearer the dust source regions in western New South Wales. At all these locations, the sky was observed to turn an orange-red color with a significant reduction in solar radiation reaching the surface being readily apparent. Along the southern coast of Australia at YMML and YPAD, no dust signature is present in the surface visibility or humidity data, indicating that all dust associated with this event is being transported north and northeastward away from these locations. The overall lag in visibility change from south to north allows us to estimate the speed at which the dust plume was moving northward and dispersing. Using the time of the initial drop in visibility as a guide, we find that the dust plume was traveling northward at speeds in excess of 20 $\mathrm{m} \cdot \mathrm{s}^{-1}$, meaning that it traversed the continent in less than two days.

One goal of this work is to determine the magnitude of the dust aerosol radiative effects and whether they can be recorded using observational data. It has been shown through observational and modeling studies that dust aerosols can either cool or warm the atmosphere depending upon surface albedo, water vapor, and dust aerosol properties [2], [10], [11]. Observations from ground instruments near Sydney noted a maximum in the

particle size distribution between 1.0 and 10.0 μm, with total particle mass concentrations (all sizes) of up to 578 $\mu g \cdot m^{-3}$ and mineral type mostly composed of silicates [12]. Yang *et al.* [11] noted that, for surface albedo greater than approximately 0.35, the shortwave cooling transitions to surface warming due to increased scattering between surface and aerosol layer. However, this threshold was not reached at the coastal sites of YBCG, YBTL, and YWLM where surface albedos from MODIS are only between 0.05 and 0.08. Therefore, a cooling effect at the surface is expected at these observation sites. Further inland near YBMA, the surface albedo was 0.1 but increased to near 0.25 near the dust source. Only in this location may warming come close to overwhelming surface cooling.

To determine if we are seeing aerosol radiative effects in this example, we first analyze the time series of temperature and dew point from six observation sites throughout central and eastern Australia (Figs. 1 and 3). For stations YBTL, YBCG, YWLM, and YBMA, a large decrease in dew point occurred at the same time as the decrease in visibility noted earlier (Fig. 3). The primary cause of the decrease in temperature and humidity is the advection of a cooler and dryer airmass into these areas after passage of the cold front (along which the dust aerosols have converged). Several previous studies have also noted the apparent collocation of dust aerosols and dry air (e.g., [13]), which is consistent with the dryer air generally present near the source regions of dust aerosols. The relationship between dust aerosols and surface temperature is not readily apparent. Along the east coast of Australia, the average diurnal temperature change during this time period has the maximum temperatures occurring around 0400 UTC with minimums occurring around 2000 UTC. The most apparent change in temperature corresponding to the arrival of the dust plume occurs at YBCG (Fig. 3). During the first hour after the rapid decrease in surface visibility, a temperature rise of approximately 7 °C was observed, followed by a surface temperature decrease of more than 10 °C during the following 8-h period between 0400 UTC and 1200 UTC. The average diurnal temperature change cannot account for these differences as it was a total of ~ 5 °C the day before. The spike in temperature at the moment of arrival of the dust plume is very interesting and could be a result of the convergence of warm air just ahead of the cold front and its associated dust plume. However, the CAA behind the cold front quickly reduces temperature, and it continues to decrease after 1400 UTC when visibility returned to normal. The primary source for the cooler air lies in southern Australia and corresponds to a region of persistent cloud cover that exists between 22 and 24 September, which can be seen in Fig. 1(a). The cloud cover acts to cool the surface compared to clear-sky conditions, and since they lie behind the cold front, they are likely to increase the strength of the cold pool of air being advected northward.

A similar pattern of rapid warming of 5 °C, followed by cooling of > 10 °C, was also observed further west at YBMA, indicating similar synoptic conditions present along much of the frontal boundary. Unlike YBCG, surface temperature appeared to recover somewhat around the time visibility improved before rapidly decreasing again. However, this secondary decrease was primarily due to the onset of nightfall and loss of solar radiation at the surface. Interestingly, temperature anomalies at the other two eastern Australian stations of YBTL and YWLM were much smaller despite the presence of the visibility and dew-point signatures corresponding to the passage of the dust plume and cold front. At YWLM, cloud cover is present until 24 September, limiting potential temperature changes from either dust aerosols or passage of the cold front. Further west at YBTL, the thickness of the dust plume and strength of the cold front were weakest, producing more limited temperature changes. In addition, the impact of smoke from the ongoing fire to the south of this site could be influencing atmospheric characteristics.

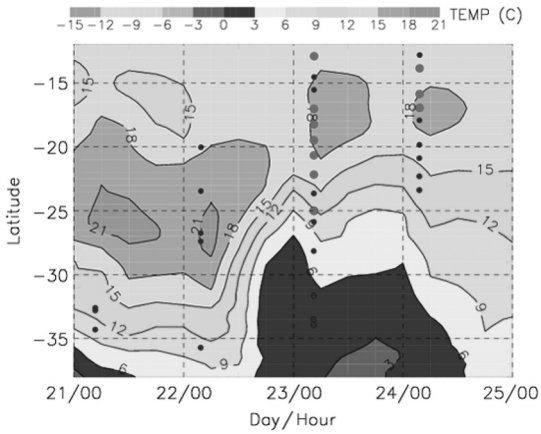

Fig. 4. GFS 850-hPa temperature (in degree Celsius) zonally averaged between 142° and 152° E every 6 h between 21 and 25 September. Locations where Aqua AOT > 0.5 along this path are plotted in maroon, and those where AOT > 1.0 are plotted in red.

Above the surface layer, larger temperature changes appear to occur corresponding to the passage of the dust plume. Fig. 4 shows the GFS 850-hPa temperature zonally averaged between 142° and 152° E at six-hourly intervals between 21 and 25 September. This level roughly corresponds to the height of the initial dust plume seen on the CALIPSO data in Fig. 2(a). Also shown are locations and times where AOT > 0.5 or > 1.0 from MODIS across the same region. The AOT data show that the concentration of dust aerosols increases significantly from 21 to 23 September, with the area between $-27°$ and $-17°$ S often having AOT > 1.0 at the latter date. The northward movement of the dust plume can also be seen, with the maximum AOT values spreading northward as a function of time, while high AOT values further southward become less common, with no AOT > 0.5 below $-25°$ S by 24 September.

A major temperature change event occurs after 1200 UTC 22 September. Temperature at 850 hPa decreased by over 10 °C over a period of less than 6 h between $-35°$ and $-28°$ S. Radiosonde data from near Brisbane were consistent with the GFS model output. The cold pool remained in place until at least 1200 UTC 24 September. Further north, temperatures remain warmer, mostly > 15 °C. Temperatures throughout the 1000–850-hPa layer generally cool from south to north in the eastern half of Australia, with cooling generally occurring behind the initial band of thick dust noted in Fig. 1(a). From these data, it is clear that cooling temperatures follow behind the dust plume, while a temperature maximum seems to exist near the location of the highest AOT values just prior to initial passage of the boundary (and consistent with the temperature

rise observed at this time from several surface stations). Even though we are likely seeing a dust-induced cooling event at the surface and aloft, it is only a small part of the overall surface temperature trends present. How small requires the use of radiative transfer modeling to estimate temperature changes given the observed aerosol properties.

To better estimate the amount of temperature change occurring as a result of *only* dust aerosol radiative effects, we use Fu-Liou radiative transfer model output [14] combined with the observed dust aerosol and surface albedo properties from MODIS and CALIPSO. Aerosol and aerosol-free fluxes are computed at the location of each surface station shown in Fig. 1 near the time corresponding to the sharp decrease in observed surface visibility. No computation is made for the two sites (YMML and YPAD) where no significant change in visibility was observed. Modeling results indicate a net (SW+LW) cooling rate of less than 1 °C per day at the surface up to the dust layer for the four remaining locations. Above the aerosol layer at 2 km, a warming rate of up to 2 °C per day was estimated. These values are much smaller than the observed temperature changes, particularly considering that the estimate heating or cooling rates are less than 2 °C *for an entire one-day period*. It is possible that the radiative transfer model is somewhat underestimating the aerosol effects, but even a doubling of the model estimate would not come close to explaining the temperature trends observed in the data. Thus, it is clear that dust aerosol radiative effects only contribute a small portion of the temperature changes being observed during this event. Synoptic effects such as CAA behind a rapidly propagating cold front are the dominant factor in temperature trends being observed, with dust radiative effects only acting to reenforce what is already happening. Much higher resolution atmospheric modeling data are required along with models that can be run with and without the dust storm occurring to close the loop on precisely quantifying this relationship for dust storms such as these.

IV. Conclusion

Analysis of the 22–24 September 2009 dust storm in eastern Australia has revealed several interesting phenomena associated with dust aerosols and the surrounding environment. The progression of this historic dust storm was evident from satellite-based sensors such as MODIS and CALIPSO. These observations showed the northward progression of a dust storm through central Australia and eventually toward New Zealand. The dust aerosol layer height was not constant and was greatest along the leading edge of the dust (2 km) and decreased in height further southward (< 1 km). This change in dust height was attributed to the rapid movement of the cold front and convergence of the dust along and over the cool pool of air as it progressed northward.

Meteorological observations also show the progression of the cold front and dust plume, primarily in the form of rapid decreases in atmospheric humidity and visibility. Dew point decreased more than 20 °C at YBTL and YCBG with visibilities dropping to below 2 km in some instances from the clear-sky value of 10 km. A sudden increase followed by a longer decrease in surface temperature was observed at two sites (YBML and YBCG) after the passage of the initial dust plume. A similar decrease occurred aloft near 850 hPa following passage of the dust layer. However, no surface temperature change was observed at other locations such as YBTL calling into question the significance of possible aerosol radiative effects in this example. Radiative transfer modeling indicates a dust aerosol radiative effect on the order of 1 or 2 °C per day, which represents a change temperature an order of magnitude smaller than measured. The primary factor in the changing surface conditions appears to be a result of the passage of the surface cold front and CAA behind it. However, surface layer cooling due to dust aerosol radiative effects may very well be reenforcing the cold pool as it progressed northward. Future research will assess this question using more dust storm examples coupled with mesoscale modeling comparisons to better quantify the effects of dust storms on surrounding atmospheric conditions.

Acknowledgment

The CALIPSO data were obtained through the NASA Langley Distributed Active Archive Systems, and the MODIS data were obtained from the Atmospheric Archive and Distribution System.

References

[1] J. Huang, Q. Fu, J. Su, Q. Tang, P. Minnis, Y. Yi, and Q. Zhao, "Taklimakan dust aerosol radiative heating derived from CALIPSO observations using Fu-Liou radiation model with CERES constraints," *Atmos. Chem. Phys.*, vol. 9, no. 12, pp. 4011–4021, Jun. 2009.

[2] C. Perez, S. Nickovic, G. Pejanovic, J. M. Baldasano, and E. Ozsoy, "Interactive dust-radiation modeling: A step to improve weather forecasts," *J. Geophys. Res.*, vol. 111, p. D16 206, 2006, DOI: 10.1029/2005JD006717.

[3] S. A. Christopher and T. A. Jones, "Dust radiative effect over global oceans," *IEEE Geosci. Remote Sens. Lett.*, vol. 5, no. 1, pp. 74–77, Jan. 2008.

[4] A. Zhu, V. Ramanathan, F. Li, and D. Kim, "Dust plumes over the Pacific, Indian, and Atlantic oceans: Climatology and radiative impact," *J. Geophys. Res.*, vol. 112, p. D16 208, 2007, DOI: 10.1029/2007JD008427.

[5] G. McTainsh, Y. C. Chan, H. McGowan, J. Leys, and K. Tews, "The 23rd October 2002 dust storm in eastern Australia: Characteristics and meteorological conditions," *Atmos. Environ.*, vol. 39, no. 7, pp. 1227–1236, Mar. 2005.

[6] L. A. Remer, R. G. Kleidman, R. C. Levy, Y. J. Kaufman, D. Tanré, S. Mattoo, J. V. Martins, C. Ichoku, I. Koren, H. Yu, and B. N. Holben, "Global aerosol climatology from the MODIS satellite sensors," *J. Geophys. Res.*, vol. 113, p. D14 S07, 2008, DOI: 10.1029/2007JD009661.

[7] M. Vaughan, S. Young, D. Winker, K. Powell, A. Omar, Z. Liu, Y. Hu, and C. Hostetler, "Fully automated analysis of space-based lidar data: An overview of the CALIPSO retrieval algorithms and data products," *Proc. SPIE*, vol. 5575, pp. 16–30, 2004.

[8] S. Moorthi, H.-L. Pan, and P. Caplan, Changes to the 2001 NCEP operational MRF/AVN global analysis/forecast system, Silver Spring, MD, 2001, Tech. Procedures Bull. 484, 14 pp. [Online]. Available: http://205.156.54.206/om/tpb/484.htm

[9] J. I. Brennan, Y. J. Kaufman, I. Koren, and R.-R. Li, "Aerosol–cloud interaction—Misclassi?cation of MODIS clouds in heavy aerosol," *IEEE Trans. Geosci. Remote Sens.*, vol. 43, no. 4, pp. 911–915, Apr. 2005.

[10] F. Patadia, E. Yang, and S. A. Christopher, "Does dust change the clear sky top of atmosphere shortwave flux over high surface reflectance regions?" *Geophys. Res. Lett.*, vol. 36, p. L15 825, 2009, DOI: 10.1029/2009GL039092.

[11] E. Yang, P. Gupta, and S. A. Christopher, "Net radiative effect of dust aerosols from satellite measurements over Sahara," *Geophys. Res. Lett.*, vol. 36, p. L18 812, 2009, DOI: 10.1029/2009GL039801.

[12] M. Radhi, M. A. Box, G. P. Box, and D. D. Cohen, "Size-resolved chemical composition of the Sydney dust storm," *J. Air Quality Clim. Change*, 2010, submitted for publication. AQ5

[13] J. P. Dunion and C. S. Velden, "The impact of the Saharan air layer on Atlantic tropical cyclone activity," *Bull. Amer. Meteorol. Soc.*, vol. 85, no. 3, pp. 353–365, Mar. 2004.

[14] Q. Fu and K. N. Liou, "Parameterization of the radiative effect properties of cirrus clouds," *J. Atmos. Sci.*, vol. 50, no. 13, pp. 2008–2025, Jul. 1993.

AUTHOR QUERIES

AUTHOR PLEASE ANSWER ALL QUERIES

AQ1 = Occurrences of "day^{-1}" were changed to "per day." Please check if OK.
AQ2 = Please provide the expanded form of the acronym "ACMAP" if applicable.
AQ3 = Please check if the intended meaning of the sentence was retained.
AQ4 = Please check if the intended meaning of the sentence was retained.
AQ5 = Please provide publication update in Ref. [12].

END OF ALL QUERIES